Substrate Diffusion within Biofilms Significantly Influencing the Electron Competition during Denitrification

Yuting Pan[1], Yiwen Liu[2,*], Lai Peng[3], Huu Hao Ngo[2], Wenshan Guo[2], Wei Wei[2], Dongbo Wang[4], Bing-Jie Ni[2,*]

[1]Department of Environmental Science and Engineering, College of Architecture and Environment, Sichuan University, Chengdu, Sichuan 610065, China

[2]Centre for Technology in Water and Wastewater, School of Civil and Environmental Engineering, University of Technology Sydney, Sydney, NSW 2007, Australia

[3]School of Resources and Environmental Engineering, Wuhan University of Technology, Luoshi Road 122, Wuhan, Hubei, 430070, China

[4]Key Laboratory of Environmental Biology and Pollution Control, College of Environmental Science and Engineering, Hunan University, Changsha, 410082, China

***Corresponding authors:**

Dr. Yiwen Liu, Tel.: +61 295149068; E-mail: Yiwen.liu@uts.edu.au

Dr. Bing-Jie Ni, Tel.: +61 295147401; E-mail: bingjieni@gmail.com

Abstract

A common and long-existing operational issue of wastewater denitrification is the unexpected accumulation of nitrite (NO_2^-) that could suppress the activity of various microorganisms involved in biological wastewater treatment process and nitrous oxide (N_2O) that could emit as a potent greenhouse gas. Recently, it has been confirmed that the accumulation of these denitrification intermediates in biological wastewater treatment process is greatly influenced by the electron competition between the four denitrification steps. However, little is known about this in biofilm systems. In this work, we applied a mathematical model that links carbon oxidation and nitrogen reduction processes through a pool of electron carriers, to assess electron competition in denitrifying biofilms. Simulations were performed comprehensively at seven combinations of electron acceptor addition scheme (i.e., simultaneous addition of one, two or three among nitrate (NO_3^-), NO_2^-, and N_2O) to compare the effect of electron competition on NO_3^-, NO_2^- and N_2O reduction. Overall, the effects of substrate loading, biofilm thickness and effective diffusion coefficients on electron competition are not always intuitive. Model simulations show that electron competition was intensified due to the substrate load limitation (from 120 to 20 mg COD/L) and increasing biofilm thicknesses (from 0.1 to 1.6 mm) in most cases, where electrons were prioritized to nitrite reductase because of the insufficient electron donor availability in the biofilm. In contrast, increasing effective diffusion coefficients did not pose a significant effect on electron competition and only increased electrons distributed to nitrite reductase when both NO_2^- and N_2O are added.

45

TOC

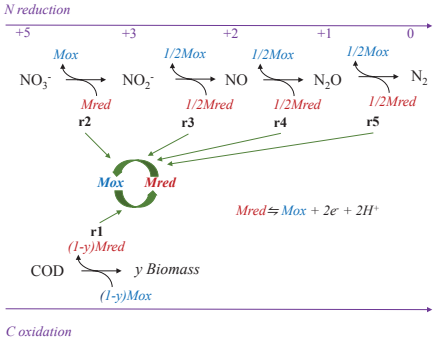
N reduction
+5
+3
+2
+1
0
Mox
1/2Mox
1/2Mox
1/2Mox
NO3-
NO2-
NO
N2O
N2
Mred
1/2Mred
1/2Mred
1/2Mred
r2
r3
r4
r5
Mox
Mred
Mred⇋ Mox + 2e- + 2H+
r1
(1-y)Mred
COD
y Biomass
(1-y)Mox
C oxidation

46

1. Introduction

Denitrification is a widely used process in wastewater treatment plant to achieve nitrogen removal. The complete denitrification process consists of NO_3^- reduction to nitrogen gas (N_2), with NO_2^-, nitric oxide (NO) and N_2O as inevitable intermediates [1]. A common operational issue of wastewater denitrification is the unexpected accumulation of NO_2^-, which could suppress the activity of various microorganisms involved in biological wastewater treatment process and thus deteriorate the effluent quality [2]. Recently, the accumulation and emission of another inevitable denitrification intermediate, N_2O, has aroused great concern and attention, as N_2O is a potent greenhouse gas with a global warming effect of ca. 300 times of carbon dioxide [3] and the dominant ozone-depleting substance emitted in the 21st century [4].

Recently, it has been confirmed that the accumulation of these denitrification intermediates is greatly influenced by the electron competition between the four denitrification steps, i.e. NO_3^- to NO_2^-, NO_2^- to NO, NO to N_2O and N_2O to N_2 [5-7]. This is because the four denitrification steps take electrons from a common electron source, and therefore the relative ability of each denitrification step to compete for electrons would regulate the electron distribution among the four denitrification steps and thus the accumulation of the denitrification intermediate [8]. Further, other environmental factors, such as pH, may exert differential effect on the activity of denitrification enzymes and lead to changes of their ability to compete for electrons [9, 10]. Therefore, a better understanding of the electron competition process would give insights to the mechanisms

of denitrification intermediates accumulation, and help to develop better operational strategy of wastewater denitrification.

Up to date, the reported investigations of electron competition have been focused on the suspended-growth (including both pure and mixed culture) system such as activated sludge process [5, 11, 12]. There is still a lack of knowledge about the attached-growth system, such as the moving bed biofilm reactor (MBBR), integrated fixed-film activated sludge (IFAS), denitrifying filters, and granular sludge, which possess a large wastewater treatment market. A noteworthy process feature of biofilm processes compared to activated sludge processes is the fact that the performance of biofilm processes is often diffusion limited, while the process kinetics for the activated sludge process are generally characterized by the bulk liquid concentrations. Thus, biofilm processes may behave differently with respect to electron competition and denitrification intermediates accumulation in contrast to suspended-growth systems. In particular, the diffusion of intermediates from one zone of the biofilm to another would lead to zones of certain intermediates (e.g., NO_2^- or N_2O) formation or consumption transformations that would not exist in suspended growth systems.

To investigate the electron competition process in biofilms, the experimental work require measuring NO_3^-, $NO_2^-$and N_2O reduction at multiple points at different layers in biofilms, this could be quite challenging considering the structure complexity of the real biofilm system. Mathematical models are widely applied in biofilm systems and denitrification systems [13], and have been proved to be useful tools to study new process

and provide strong support for the understanding and optimization of new technologies as already demonstrated previously [14, 15]. Recently, we have developed and validated a model, namely Activated Sludge Model for Indirect Coupling of Electrons (ASM-ICE) [16] to describe the electron competition process in denitrification systems, which has been successfully applied to reveal the mechanisms of N_2O formation and reduction in denitrifying biofilms [17]. However, the detailed electron competition process in denitrifying biofilms is still not fully understood.

Therefore, the main objective of this work is to perform a model-based assessment of electron competition process during wastewater denitrification in biofilm systems, through implementing ASM-ICE model in biofilms. In this study, we limit the biofilm system to denitrification biofilm so that the electron competition process is evident. The impacts of key operational parameters, including influent surface loading, biofilm thickness and mass transfer coefficient on the electron competition process and N_2O accumulation are investigated.

2. Materials and Methods

2.1 Analysis of ASM-ICE model

The ASM-ICE model was developed and validated to describe the electron competition process using suspended-growth culture in bulk liquid systems [16]. The key difference between ASM-ICE and the previous denitrification models, e.g., ASMN [18], is that the proposed model links carbon oxidation and nitrogen reduction processes through a pool

of electron carriers, while the previous denitrification models directly couple the two processes.

The ASM-ICE model includes five reactions, r1- r5 (Figure 1), with r1 describing the carbon oxidation process and r2 - r5 describing the nitrogen oxides (NO_3^-, NO_2^-, NO and N_2O) reduction processes. Electron carriers, with *Mox* representing oxidized from of electron carriers and *Mred* (*Mred* $\leftrightharpoons$ *Mox* + $2e^-$ + $2H^+$) representing reduced form of electron carriers, are used in ASM-ICE model to link the carbon oxidation process and the nitrogen oxides reduction processes. The carbon oxidation process (r1) provide the electrons to *Mox* and reduce it back to *Mred,* while the nitrogen reduction process (r2 to r5) draw electrons from *Mred* and oxidize Mred back to *Mox.* The four nitrogen oxides reduction steps possess different abilities to compete for *Mred*, which is mainly affected by their affinity constants for *Mred.* It is believed that NO reductase has the highest affinity constants, mainly due to NO reduction is usually prioritized by bacteria to avoid its toxicity [13]. Hence, the NO concentrations and rates will not be specifically addressed in detail in this work due to the fact that NO would be quickly consumed and maintain at near-zero concentrations. Experimental results also suggested that nitrite reductase has higher ability to compete for electrons than nitrate and N_2O reductase. Model components are shown in Table S1 in Supporting Information (SI). Table S3 in the SI shows the model matrices with kinetics and stoichiometrics.

2.2 Denitrifying biofilm model

In this work the electron competition during denitrification process is incorporated into biofilm system, with the ASM-ICE model being integrated into a biofilm compartment of the software package (AQUASIM) for aquatic systems [19]. AQUASIM is a program, in which the spatial configuration of a model system can be represented by compartments, which are connected by links. The program allows the user to define an arbitrary number of substances to be modelled and it is extremely flexible in the formulation of transformation processes. It is a finite difference method (FDM)-based software. Execution of a simulation is equivalent to numerically integrating a system of ordinary and partial differential equations in time and simultaneously solving the algebraic equations [19]. The biofilm reactor was modelled through consisting of two different compartments, namely the biofilm and bulk liquid. The bulk volume and biofilm surface of the reactor is 4 L and 50 dm^2, respectively. The influent flow rate was set at 4 L/day, containing COD and nitrogen oxides. The biofilm compartment is limited to denitrifying biofilms, so that the electron competitions between the nitrogen reductases are evident. For simplicity, a one-dimensional stationary biofilm with fixed thickness was assumed in all cases, without any biomass growth, attachment or detachment. Denitrifiers were considered to be uniformly distributed throughout the biofilm, without diffusive mass transport of biomass in the biofilm matrix. This approach has been well applied in literature for describing biofilm systems [14, 17]. The water fraction of the biofilm matrix is kept constant at 0.8, while the biomass density is 50 g/L. Parameters regarding the mass transfer coefficients for NO_3^-, NO_2^-, NO, N_2O and COD are adopted from Haynes [20]. Twenty grid points in the biofilm were selected for calculation in specified compartment. A simulation was defined for an active calculation with 2,000 steps of 1 day, which was

long enough to assure steady-state conditions. The biofilm and mass transfer parameters are shown in Table S2 in the SI.

2.3 Modeling approach and simulation scenarios

Previously well-established parameter values of electron competition during denitrification in ASM-ICE model that have been verified with experimental data are used in this simulation study. Therefore, we directly adapt these parameter values and kinetic rates into the model and evaluate the substrate and microbial interactions in the denitrification biofilm system, which has been demonstrated to be a valid method in previous studies [17, 21-23]. It should be noted that the applied set of parameters in this study may not have a universal suitability for all denitrifiers due to the fact that the kinetic rates may vary among different types of denitrifiers. However, the simulation results of this work under different operational conditions are still useful for the understanding of electron competition in denitrification biofilm due to the fact that the possible variation of biodegradation rates would not alter the overall trends based on the applied model structure. Table S2 in the SI shows the definitions, values, units and sources of all parameters used in the biological reaction model. Model simulations are then performed under different operational conditions, namely COD loading, biofilm thickness and effective diffusion coefficients (i.e., D_e/D, reduction factor of diffusion coefficients in the biofilm compared to the aqueous phase).

Methanol and various nitrogen oxides are supplied to the mixed liquor in each test. The COD concentration in the influent ranges from 20 to 120 mg/L. The nitrogen oxides are supplied according to the electron acceptor addition scheme (as shown in Table 1), with

the concentration in the influent being 20 mg N/L of each nitrogen oxide. Overall, seven different electron acceptor addition method (i.e., simultaneous addition of one, two or three among NO_3^-, NO_2^-, and N_2O) were applied, to provide data to compare the effect of electron competition on NO_3^-, NO_2^- and N_2O reduction. Simulations were then performed at different combinations of electron acceptor addition scheme, influent COD concentration, biofilm thickness and effective diffusion coefficients to investigate 1) the effect of COD concentration on electron competition; the effect of biofilm thickness on electron competition; and 3) the effect of mass transfer on electron competition in biofilm.

Four different scenarios are considered (Table 1). The standard simulation scenario (Scenario 0 of Table 1) is firstly performed to assess the potential electron competition in biofilm with the initial COD concentration at 90 mg/L, biofilm thickness at 1mm and D_e/D at 0.5. Scenarios 1- 3 in Table 1 examine the effects of influent COD concentration (varied between 20-120 mg/L), biofilm thickness (0.1-1.6 mm) and mass transfer (D_e/D varied between 0.2-0.8) on electron competition in biofilms, respectively. In each simulation, e.g., the influent COD concentration of 20 mg/L of Scenario 1, the simulation were performed at seven different electron acceptor addition schemes, i.e. a) NO_3^- alone, b) NO_2^- alone, c) N_2O alone, d) NO_3^- and NO_2^-, e) NO_3^- and N_2O, f) NO_2^- and N_2O, and finally g) NO_3^-, NO_2^- and N_2O, to evaluate the electron distribution between different nitrogen reduction reaction.

3. Results

3.1 Electron competition in denitrifying biofilm

With the surface loading, biofilm thickness and effective diffusion coefficient set as in Scenario 0 (standard case), the model was first used to predict the nitrogen reduction in the biofilm to establish an overall picture of the electron competition process in the denitrifying biofilm.

In general, the nitrogen compounds gradually reduced in the biofilm. For example, as shown in Figure 2-a, when only NO_3^- was added, the NO_3^- concentration gradually reduced from 20 mg N/L at surface of the biofilm to around 6 mg N/L at around 0.6 mm of the biofilm and then gradually reduced to around 2 mg N/L at the bottom in the biofilm. There were still some NO_3^- left at the bottom of the biofilm, since COD was completely consumed at around 0.2 mm of the biofilm as shown in Figure 2-h. In comparison, when NO_2^- was added alone (Figure 2-b), the NO_2^- concentration gradually reduced from 20 mg N/L at the surface of the biofilm to around 0 mg N/L at 0.25 mm of the biofilm, while COD was still in excess at 0.25 mm (Figure 2-h).

There were highly different accumulations of N_2O in Figure 2-a, 2b and 2d. In Figure 2-a (NO_3^- added alone), N_2O only accumulated to around 0.005 mg N/L, while in Figure 2-b (NO_2^- added alone), N_2O accumulated to around 0.015 mg N/L. The highest N_2O accumulation occurred in Case d (both NO_3^- and NO_2^- were added), up to almost 0.1 mg N/L, which is 20 times higher than that of Case a (Figure 2).

One coherent observation was that the nitrogen oxide compound affects each other's reduction rate. Take NO_3^- reduction for example, NO_3^- were added in Case a (Figure 2-a),

Case d (Figure 2-d) and Case g (Figure 2-g). The highest NO_3^- reduction rate was observed in Case a when NO_3^- was added alone, with the NO_3^- concentration at around 2 mg N/L at the bottom of the biofilm. In comparison, the lowest NO_3^- reduction rate was observed in Case g when three electron acceptors were all presented in the influent, with the NO_3^- concentration at around 17 mg N/L at the bottom of the biofilm. Similar trend also applies to NO_2^- and N_2O reduction. This is not surprising, as the more electron acceptors were presented, the more severe electron competition would occur [24]. Therefore, the rate of each denitrification step would be affected, clearly demonstrating the electron competition in denitrifying biofilm.

3.2 Impact of COD loading on electron competition in denitrifying biofilm

Considering that the availability COD would affect the supply of electron donor, the effect of COD concentration on electron distribution in denitrifying biofilm was investigated in Scenario 1 (Table 1). In this scenario, the COD concentrations in the influent were tested against 20, 40, 80, 90, 100, 110 and 120 mg/L. The simulation of each COD concentration was performed at seven different electron acceptor addition schemes, i.e. a) NO_3^- alone, b) NO_2^- alone, c) N_2O alone, d) NO_3^- and NO_2^-, e) NO_3^- and N_2O, f) NO_2^- and N_2O, and finally g) NO_3^-, NO_2^- and N_2O (as shown in Table 1).

Three electron acceptor addition schemes (Case a, b and d) were presented in detail in Figure 3, including the simulation results of nitrogen oxides profile, COD profile and electron distribution pattern, to reveal the effect of COD concentration on electron distribution in the denitrifying biofilm system.

Case a: When NO_3^- was added alone as electron accepter, the electron distribution among nitrate reductase (Nar), nitrite reductase (Nir) and N_2O reductase (Nos) remained at a constant level (Figure 3-IV). The corresponding COD consumption profile (Figure 3-III) reveals that COD was either in excess at the bottom of the biofilm or completely consumed at outer layer of the biofilm. These results together suggest that when NO_3^- was added alone, the electron distribution was not affect by the COD loading.

Case b: When only NO_2^- was added as electron accepter, the electron distribution presented two distinct patterns (Figure 3-iv). The electrons distributes to Nir accounted for around 85%, when the influent COD was below 40 mg/L. Contrarily, when the influent COD was above 80 mg/L, the electrons distributes to Nir only accounted for around 65%. By analyzing the COD to N ratio, it is obvious that the COD was not sufficient for complete nitrite denitrification when COD was below 40 mg/L and thus the electron completion would be more severe than those tests with sufficient influent COD for complete NO_2^- reduction, i.e. COD concentration above 80 mg/L.

Case d: when both NO_3^- and NO_2^- were added as electron accepter, COD was not enough for NO_3^- and NO_2^- reduction in all the cases (As shown in Figure 3-3). However, the COD influent concentration would still affect the N_2O accumulation. As shown in Figure 3-1 and Figure 3-2, the N_2O accumulates to around 0.15 mg/L with influent COD at 20 mg/L and only about 0.01 mg/L with influent COD at 120 mg/L. Similar to Case b

(Figure 3-iv), less COD present in the influent would lead to more electrons distributed to Nir (Figure 3-4)

The electron distribution patterns of the 7 electron additions schemes are summarized in Figure S1 in the SI. In general, all the results suggested that the electron distribution was significantly affected by the COD loading in most of the cases. A coherent trend is that when COD loading reduced from 120 mg/L to 20 mg/L, the electrons distributed to nitrite reductase would increase, except for Case e (adding NO_3^- and N_2O). This is likely due to that the reduced COD loading would decrease the supply of electron donor, and thus intensify the electron competition. Nitrite reductase (Nir), with affinity constant to electrons of 0.00040 mmol/(mmol biomass), has higher ability to compete for electrons than nitrate reductase (Nar) and N_2O reductase (Nos) with their affinity constants being 0.0046 and 0.0032 mmol/(mmol biomass), respectively [16]. Therefore, the electrons distributed to NO_2^- increased when COD loading gradually reduced. In Case e, NO_2^- was resulted from NO_3^- reduction. The reduced COD loading led to more electrons to N_2O reduction and thus less electrons were distributed to Nir.

3.3 Impact of biofilm thickness on electron competition in denitrifying biofilm

Considering that the biofilm thickness would affect various aspects of substrate/product distribution and diffusion in biofilm systems, the effect of biofilm thickness on electron competition was explored in Scenario 2 (Table 1). In this scenario, with other parameters (i.e., influent COD concentration and effective diffusion coefficients) kept constant, the biofilm thicknesses were tested against 0.1, 0.4, 0.7, 1.0, 1.3 and 1.6 mm (Table 1). The

297 simulation of each biofilm thickness was performed at seven different electron acceptor
298 addition schemes as shown in Table 1.
299
300 Three electron acceptor addition schemes (Case a, b and d) were presented in detail in
301 Figure 4, including the simulation results of nitrogen oxides profile, COD profile and
302 electron distribution pattern, to reveal the effect of biofilm thickness on electron
303 distribution in the denitrifying biofilm system.
304
305 ***Case a:*** Comparing the results from Figure 4-I, II and III, it is clear that the biofilm
306 thickness would affect the NO_3^- and COD concentration profile. Greater biofilm
307 thicknesses resulted in steeper NO_3^- and COD concentration gradient in the biofilm,
308 which is probably due to better substrate penetration along the biofilm. For example,
309 when the biofilm thickness is 0.4 mm, the NO_3^- concentration only reduced by 4.5 mg/L
310 from 20 mg/L at 0.4 mm to 15.5 mg/L at 0 mm (Figure 4-I). In comparison, when the
311 biofilm thickness is 1.6mm, the NO_3^- concentration reduced by 13.5 from 20 mg/L at
312 1.6mm to 7 mg/L at 1.2mm (Figure 4-II). Figure 4-III reveal that COD was either in
313 excess at the bottom of the biofilm or completely consumed at the outer layer of the
314 biofilm. Figure 4-IV indicates that the biofilm thickness has no significant influence on
315 the electron distribution when only NO_3^- is added.
316
317 ***Case b:*** Similar to Case a, greater biofilm thicknesses had steeper NO_2^- and COD
318 concentration gradient (Figure 4-i and ii). COD was in excess in all the biofilm ranges, as
319 indicated by Figure 4-iii. Figure 4-iv reveals that greater biofilm thicknesses led to less

electrons distributed to Nir. Therefore, the trend is regardless of the COD concentration, and only the biofilm thickness affects the electron distribution.

Case d: Similar to Cases a and b, greater biofilm thicknesses had steeper NO_3^-, NO_2^- and COD concentration gradient (Figure 4-1 and 2). The COD profile shows that when the biofilm thickness is 1.6 mm, COD was completely consumed. However, when the biofilm thickness is 0.4 mm, COD was in excess at the bottom of the biofilm. The results of this case study suggest that the electron distribution is not only affected by the biofilm thickness, but also by the COD availability which is also correlated to biofilm thickness. Figure 4-4 suggests that greater biofilm thicknesses resulted in more electrons distributed to Nir.

The electron distribution patterns of the 7 electron additions schemes are compared in Figure S2 in the SI. In Case d (i.e., add NO_3^- and NO_2^-), Case e (i.e., add NO_3^- and N_2O) and Case g (i.e., add NO_3^-, NO_2^- and N_2O), greater biofilm thicknesses led to more electrons distributed to Nir, due to the insufficient COD availability in the thicker biofilm that increased electron competition. In contrast, in Case b (add NO_2^- alone) and Case f (add NO_2^- and N_2O alone), greater biofilm thicknesses resulted in less electrons distributed to Nir, as thicker biofilms had greater N_2O reduction in the deeper layer of the biofilm and more electrons were thus distributed to Nos.

3.4 Impact of mass transfer on electron competition in denitrifying biofilm

342 The different biofilms might possess different mass transfer capabilities. Compact
343 biofilm may have lower mass transfer ability. Therefore, this section explores the effect
344 of mass transfer on the electron competition (Scenario 3 in Table 1). In this scenario, with
345 other parameters (i.e., influent COD concentration and biofilm thickness) kept constant,
346 D_e/D were tested against 0.2, 0.3, 0.4, 0.5, 0.6, 0.7 and 0.8 (Table 1). The simulation of
347 each D_e/D was performed at seven different electron acceptor addition schemes as shown
348 in Table 1.
349
350 Three electron acceptor addition schemes (Case d, f and g) were presented in detail in
351 Figure 5, including the simulation results of nitrogen oxides profile, COD profile and
352 electron distribution pattern, to reveal the effect of effective diffusion coefficient on
353 electron distribution in the denitrifying biofilm system.
354
355 ***Case d:*** when both NO_3^- and NO_2^- were added as electron accepter, COD was sufficient
356 at a D_e/D of 0.8 (Figure 5-III). When D_e/D was lower than 0.8, COD was insufficient for
357 nitrogen oxide reduction and higher accumulation of N_2O was found in the biofilm, i.e.,
358 10 mg-N/L at a D_e/D of 0.3 vs 7 mg-N/L at a D_e/D of 0.8 (Figure 5-I and II), probably
359 due to the penetration limitation of COD. However, the electron distribution pattern was
360 not substantially affected by D_e/D in Case d (Figure 3-IV).
361
362 ***Case f:*** when both NO_2^- and N_2O were added as electron accepter, COD was not enough
363 for NO_2^- and N_2O reduction in all the cases (Figure 5-iii). Similar to Case d, NO_2^-
364 concentration gradient decreased with the increased D_e/D (Figure 5-i and ii), i.e., NO_2^-

365 became zero, at 0.4 mm at a D_e/D of 0.3, and at the bottom at a D_e/D of 0.8. The electron
366 distribution pattern was substantially affected by D_e/D in Case f, i.e., greater D_e/D
367 resulted in more electrons distributed to Nir.
368
369 ***Case g:*** Similar to Case d and f, lower D_e/D had steeper NO_2^- and COD concentration
370 gradient (Figure 5-1 and 2). COD was limited in all the D_e/D ranges, as indicated by
371 Figure 5-3. In contrast to Case f, the electron distribution pattern was not substantially
372 affected by D_e/D (Figure 5-4).
373
374 The electron distribution patterns of the 7 electron additions schemes are compared in
375 Figure S3 in the SI. There is no significant change of the electron competition, except for
376 Case f when both NO_2^- and N_2O are added. In Case f, deeper penetration of NO_2^- to the
377 bottom of the biofilm as a result of increased D_e/D would consume more electrons and
378 thus more electrons were distributed to Nir.
379
380 **4. Discussion**
381 Denitrification process is an important step during biological nitrogen removal. However,
382 the unbalance between the electron supply and consumption, particularly under a limited
383 electron supplying flux, would lead to deteriorated denitrification, i.e., accumulation of
384 NO_2^- and N_2O [16]. In this work, a previously-established approach that decouples the
385 carbon oxidation with four-step nitrogen oxides reduction processes through the
386 introduction of electron carriers was applied to describe electron competition in the

different electron acceptors (i.e., simultaneous addition of one, two or three of NO_3^-, NO_2^- and N_2O) during denitrification in denitrifying biofilm.

The results clearly indicate that the mechanisms of electron competition in the denitrifying biofilms are highly different from those in suspended-growth processes [25], where NO_2^- reduction was prioritized over the other denitrification steps when electron supply became the limiting step. In a suspended-growth system without substrate diffusion, the fractions of electrons distributed to nitrite reductase increased with the decrease of electron supply rate, thus resulting in accumulation of other nitrogen oxide intermediates. This could be attributed to a higher capacity of NO_2^- reduction for electron competition under electron limiting conditions (i.e., a low S_{Mred} concentration), specifically, $K_{Mred,2}$ (S_{Mred} affinity constant for Nir) has a value that is approximately ten times lower than $K_{Mred,1}$ (S_{Mred} affinity constant for Nar) and $K_{Mred,4}$ (S_{Mred} affinity constant for Nos) [25].

A key difference between attached- and suspended-growth processes is that in a biofilm, nitrogen oxide intermediates generated during denitrification can diffuse according to substrate gradients [17]. This can further impact electron competition during denitrification in the biofilm. In particular, COD loading, biofilm thickness and effective diffusion coefficients can affect the substrate diffusion in the biofilm and in turn impact electron competition. With the increasing scarcity of electron donors in the biofilm (i.e., COD loading from 120 mg/L to 20 mg/L), the electrons distributed to nitrite reductase increased in most addition schemes in the biofilm, similar to the suspended-growth

process. However, in Case e (adding NO_3^- and N_2O), it led to a contrary trend, which could be explained by the fact that NO_2^- was not present at the beginning and more electrons were distributed to N_2O reduction compared to NO_3^- reduction if electrons were limited.

The inherent property of biofilm also altered the electron competition tendency compared to that of the suspended-growth system. Increasing biofilm thicknesses had more electrons distributed to NO_2^- reduction in most addition schemes, due to the insufficient electron donor availability in the thicker biofilm. In contrast, in Case b (add NO_2^- alone) and Case f (add NO_2^- and N_2O), less electrons distributed to Nir with the increase of biofilm thicknesses, likely due to the stronger N_2O sink as a result of greater biofilm thicknesses. In comparison, increased effective diffusion coefficients only affected electrons distributed to Nir in Case f when both NO_2^- and N_2O are added. The electrons distributed to Nir increased with the increase of effective diffusion coefficients due to the better penetration of NO_2^- to the biofilm.

The biofilm processes have been widely used in wastewater treatment plants (WWTPs), such as MBBR, IFAS, denitrifying filters, and granular sludge. Substrate diffusion limitation is often observed in biofilm processes, which may behave differently in terms of electron competition and denitrification intermediate accumulation in contrast to activated sludge processes. This study would help to understand and develop the effective strategies to reduce the accumulation of unfavorable denitrification intermediates, particularly N_2O. For a biofilm denitrifying system, alternating effective diffusion

coefficients would not significantly affect electron competition and thus alleviate the N_2O accumulation except that only NO_2^- and N_2O are presented in the influent from nitrifying reactor. In comparison, decreasing biofilm thickness would be a useful way to reduce N_2O accumulation in most cases. However, if NO_2^- alone or NO_2^- with N_2O is in the influent, on the contrary, increasing biofilm thickness would alleviate N_2O accumulation. In addition, it should be revealed that, increasing COD loading, one common strategy used to alleviate N_2O accumulation in activated sludge processes, might not still work in biofilm systems with NO_3^- alone or NO_3^- and N_2O in the influent.

The objective of this work is to provide insights into electron competition during denitrification in biofilms. Ideally, the above goal in this study would be achieved if the model could be calibrated using experimental data. This is unfortunately not possible at present due to the lack of data. We have therefore chosen to conduct a simulation study by integrating well-established models describing electron competition during denitrification. We recognize that without being validated with data, the model predictions are preliminary and remain to be verified. However, we believe the preliminary results will already support our understanding in this process. Further efforts should be devoted to conducting experimental work to support the hypotheses produced by this modeling work in future.

Acknowledgements

This study was partially funded by National Natural Science Foundation of China through project 51508355. Y. Liu acknowledges the support from the UTS Chancellor's

Postdoctoral Research Fellowship and CTWW Industry Partner & ECR Mentoring Scheme funding. B.J. Ni acknowledges the support of an Australian Research Council (ARC) Future Fellowship (FT160100195). The authors are grateful to the research collaboration.

Supporting information

Model components, parameter values and model matrices in Table S1-S3, and additional experimental data in Figure S1-S3.

Conflict of Interest Disclosure

The authors declare no conflict of interest.

References

1. Zumft, W. G., Cell biology and molecular basis of denitrification. *Microbiol. Mol. Biol. Rev.* **1997,** *61*, (4), 533-616.

2. Glass, C.; Silverstein, J., Denitrification kinetics of high nitrate concentration water: pH effect on inhibition and nitrite accumulation. *Water Res.* **1998,** *32*, (3), 831-839.

3. IPCC, Climate Change 2007: The Physical Science Basis. Contribution of Working Group I to the Fourth Assessment Report of the Intergovernmental Panel on Climate Change [Solomon, S., D. Qin, M. Manning, Z. Chen, M. Marquis, K.B. Averyt, M. Tignor and H.L. Miller (eds.)]. Cambridge University Press, Cambridge, United Kingdom and New York, NY, USA. **2007**.

4. Ravishankara, A. R.; Daniel, J. S.; Portmann, R. W., Nitrous oxide (N2O): the dominant ozone-depleting substance emitted in the 21st century. *Science* **2009,** *326*, (5949), 123-125.

5. Pan, Y.; Ni, B.-J.; Bond, P. L.; Ye, L.; Yuan, Z., Electron competition among nitrogen oxides reduction during methanol-utilizing denitrification in wastewater treatment. *Water Res.* **2013,** *47*, (10), 3273-3281.

6. Ribera-Guardia, A.; Kassotaki, E.; Gutierrez, O.; Pijuan, M., Effect of carbon source and competition for electrons on nitrous oxide reduction in a mixed denitrifying microbial community. *Process Biochem.* **2014,** *49*, (12), 2228-2234.

7. Almeida, J. S.; Reis, M. A. M.; Carrondo, M. J. T., Competition between nitrate and nitrite reduction in denitrification by *Pseudomonas fluorescens*. *Biotechnol. Bioeng.* **1995,** *46*, (5), 476-484.

8. Richardson, D.; Felgate, H.; Watmough, N.; Thomson, A.; Baggs, E., Mitigating release of the potent greenhouse gas N_2O from the nitrogen cycle - could enzymic regulation hold the key? *Trends Biotechnol.* **2009,** *27*, (7), 388-397.

9. Pan, Y.; Ye, L.; Ni, B.-J.; Yuan, Z., Effect of pH on N_2O reduction and accumulation during denitrification by methanol utilizing denitrifiers. *Water Res.* **2012,** *46*, (15), 4832-4840.

10. Thomsen, J. K.; Geest, T.; Cox, R. P., Mass-spectrometric studies of the effect of pH on the accumlation of intermediates in denitrification by *Paracoccus denitrificans*. *Appl. Environ. Microb.* **1994,** *60*, (2), 536-541.

11. Wilderer, P. A.; Jones, W. L.; Dau, U., Competition in denitrification systems affecting reduction rate and accumulation of nitrite. *Water Res.* **1987,** *21*, (2), 239-245.

12. Kucera, I.; Dadak, V.; Dobry, R., The distribution of redox equivalents in the anaerobic respiratory chain of *paracoccus* denitrificans. *Eur. J. Biochem.* **1983,** *130*, (2), 359-364.

13. Liu, Y.; Peng, L.; Ngo, H. H.; Guo, W.; Wang, D.; Pan, Y.; Sun, J.; Ni, B.-J., Evaluation of nitrous oxide emission from sulfide-and sulfur-based autotrophic denitrification processes. *Environ. Sci. Technol.* **2016,** *50*, (17), 9407-9415.

14. Sabba, F.; Picioreanu, C.; Pérez, J.; Nerenberg, R., Hydroxylamine Diffusion Can Enhance N2O Emissions in Nitrifying Biofilms: A Modeling Study. *Environ. Sci. Technol.* **2015,** *49*, (3), 1486-1494.

15. Ni, B.-J.; Pan, Y.; van den Akker, B.; Ye, L.; Yuan, Z., Full-Scale Modeling Explaining Large Spatial Variations of Nitrous Oxide Fluxes in a Step-Feed Plug-Flow Wastewater Treatment Reactor. *Environ. Sci. Technol.* **2015,** *49*, (15), 9176-9184.

16. Pan, Y.; Ni, B.-J.; Lu, H.; Chandran, K.; Richardson, D.; Yuan, Z., Evaluating two concepts for the modelling of intermediates accumulation during biological denitrification in wastewater treatment. *Water Res.* **2015,** *71*, 21-31.

17. Sabba, F.; Picioreanu, C.; Nerenberg, R., Mechanisms of nitrous oxide (N2O) formation and reduction in denitrifying biofilms. *Biotechnol. Bioeng.* **2017,** *114*, (12), 2753-2761.

18. Hiatt, W. C.; Grady, C. P. L., An updated process model for carbon oxidation, nitrification, and denitrification. *Water Environ. Res.* **2008,** *80*, (11), 2145-2156.

19. Reichert, P., AQUASIM - Computer Program for Simulation and Data Analysis of Aquatic Systems. *EAWAG, Dübendorf 1998*.

20. Haynes, W. M., *CRC handbook of chemistry and physics*. CRC press: 2014.

21. Wang, D.; Liu, Y.; Ngo, H. H.; Zhang, C.; Yang, Q.; Peng, L.; He, D.; Zeng, G.; Li, X.; Ni, B.-J., Approach of describing dynamic production of volatile fatty acids from sludge alkaline fermentation. *Bioresour. Technol.* **2017,** *238*, 343-351.

22. Sabba, F.; Picioreanu, C.; Boltz, J. P.; Nerenberg, R., Predicting N2O emissions from nitrifying and denitrifying biofilms: a modeling study. *Water Sci. Technol.* **2017,** *75*, (3), 530-538.

23. Mannina, G.; Ekama, G.; Caniani, D.; Cosenza, A.; Esposito, G.; Gori, R.; Garrido-Baserba, M.; Rosso, D.; Olsson, G., Greenhouse gases from wastewater treatment—A review of modelling tools. *Sci. Total Environ.* **2016,** *551*, 254-270.

24. Liu, Y.; Ngo, H. H.; Guo, W.; Peng, L.; Chen, X.; Wang, D.; Pan, Y.; Ni, B. J., Modeling electron competition among nitrogen oxides reduction and N2O accumulation in hydrogenotrophic denitrification. *Biotechnol. Bioeng.* **2018,** *115*, (4), 978-988.

25. Pan, Y.; Ni, B.-J.; Yuan, Z., Modeling electron competition among nitrogen oxides reduction and N2O accumulation in denitrification. *Environ. Sci. Technol.* **2013,** *47*, (19), 11083-11091.

Table Caption

Table 1: An overview of the simulation scenarios and electron acceptor addition scheme

Figure Captions

Figure 1. Simplified representation of the biochemical reactions associated with electron competition during denitrification.

Figure 2. Model simulation results of the nitrogen oxides reduction (a-g) and the COD consumption in denitrification biofilm (h). Electron acceptor addition scheme: a) Add NO_3^- alone, b) add NO_2^- alone, c) add N_2O alone, d) add NO_3^- & NO_2^-, e) add NO_3^- & N_2O, f) add NO_2^- & N_2O, and g) add NO_3^-, NO_2^- & N_2O. The surface of the sediment was defined as depth 1 mm.

Figure 3. The effect of COD concentration on nitrogen oxides reduction (I~II, i~ii and 1~2), COD consumption (III, iii and 3), and electron distribution between Nar, Nir and Nos (IV, iv and 4). I~ IV show the simulation results of Case a, with only NO_3^- presenting in the influent. i~ iv show the simulation results of Case b, with only NO_2^- presenting in the influent. 1~4 show the simulation results of Case d, with both NO_3^- and NO_2^- in the influent. The surface of the sediment was defined as depth 1 mm.

Figure 4. The effect of biofilm thickness on nitrogen oxides reduction (I~II, i~ii and 1~2), COD consumption (III, iii and 3), and electron distribution between Nar, Nir and Nos (IV, iv and 4). I~ IV show the simulation results of Case a, with only NO_3^- presenting in the

566 influent. i~ iv show the simulation results of Case b, with only NO_2^- presenting in the
567 influent. 1~4 show the simulation results of Case d, with both NO_3^- and NO_2^- in the
568 influent. The bottom of the sediment was defined as depth 0 mm.
569
570 **Figure 5.** The effect of mass transfer on nitrogen oxides reduction (I~II, i~ii and 1~2),
571 COD consumption (III, iii and 3), and electron distribution between Nar, Nir and Nos (IV,
572 iv and 4). I~ IV show the simulation results of Case d, with NO_3^- and NO_2^- presenting in
573 the influent. i~ iv show the simulation results of Case f, with NO_2^- and N_2O presenting in
574 the influent. 1~4 show the simulation results of Case g, with NO_3^-, NO_2^- and N_2O present
575 in the influent. The surface of the sediment was defined as depth 1 mm.
576

577 **Table 1:** An overview of the simulation scenarios and electron acceptor addition scheme

Scenarios	Standard conditions	Variable conditions
Scenario 0 Standard simulation	COD = 90 mg/L L_f = 1 mm D_e/D = 0.5	
Scenario 1 Effect of COD concentration on electron competition	L_f = 1 mm D_e/D = 0.5	COD=20-120
Scenario 2 Effect of biofilm thickness on electron competition	COD = 90 mg/L D_e/D = 0.5	L_f=0.1-1.6
Scenario 3 Effect of mass transfer on electron competition in biofilm	COD = 90 mg/L L_f = 1 mm	D_e/D =0.2-0.8

Electron acceptor addition scheme						
a	**b**	**c**	**d**	**e**	**f**	**g**
NO_3^-	NO_2^-	N_2O	NO_3^- NO_2^-	NO_3^- N_2O	NO_2^- N_2O	NO_3^- NO_2^- N_2O

578

579

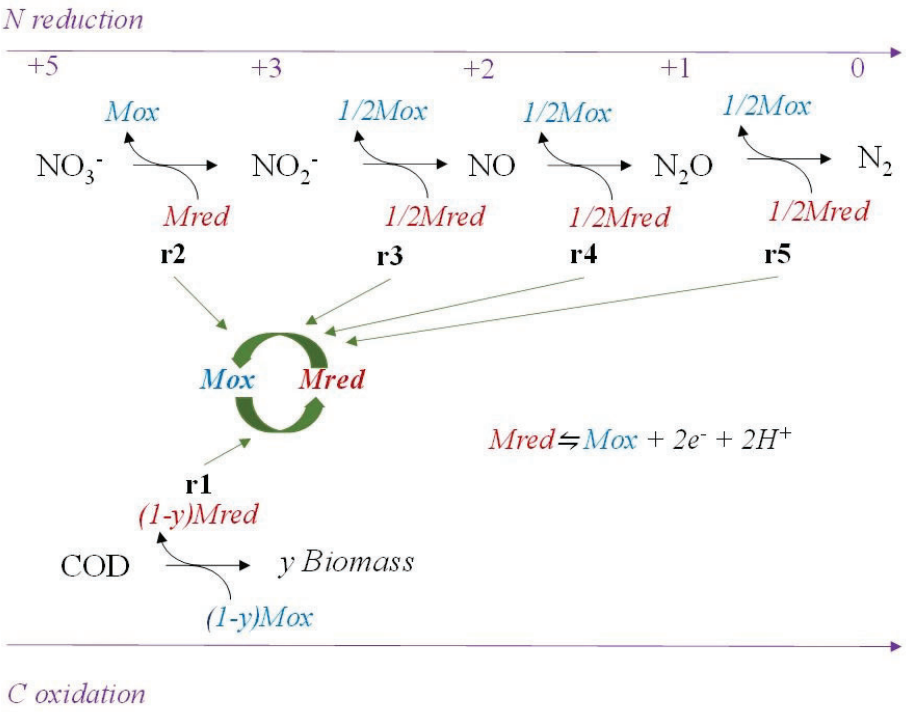

Figure 1. Simplified representation of the biochemical reactions associated with electron competition during denitrification.

247x189mm (96 x 96 DPI)

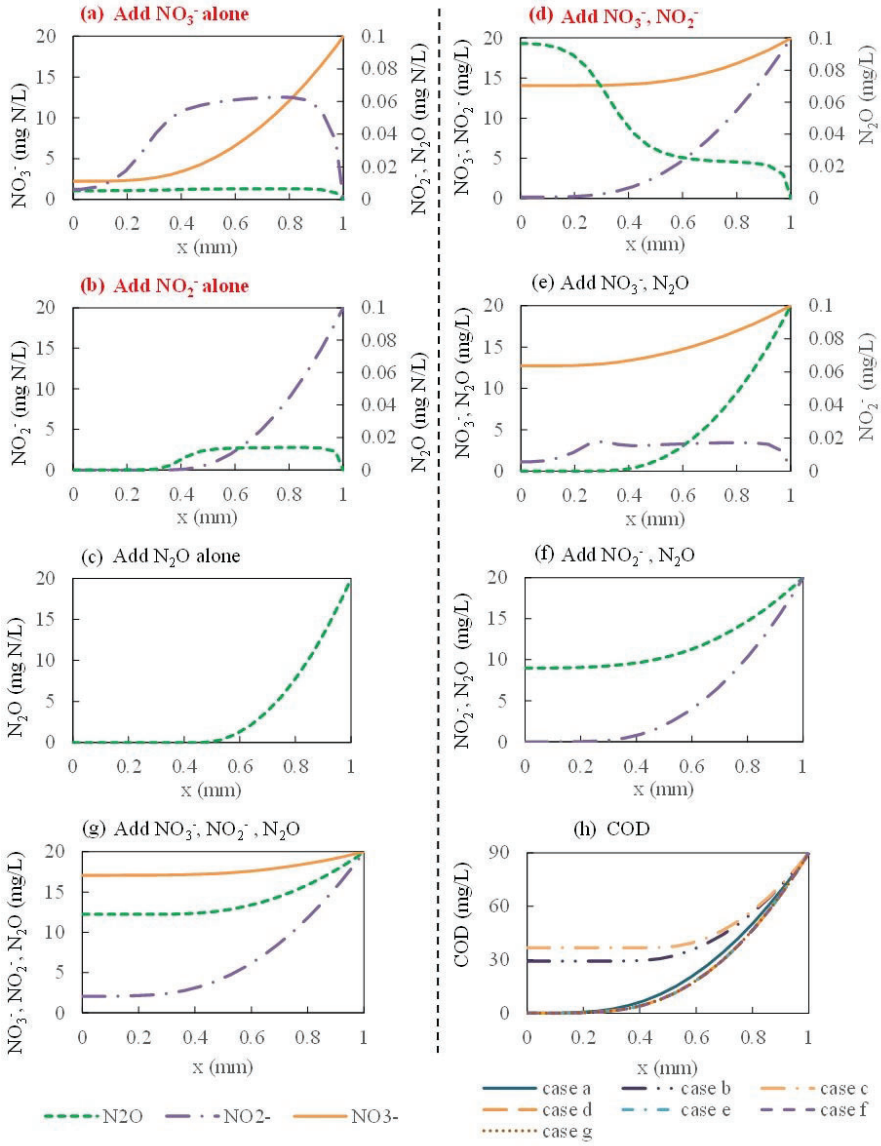

Figure 2. Model simulation results of the nitrogen oxides reduction (a-g) and the COD consumption in denitrification biofilm (h). Electron acceptor addition scheme: a) Add NO3 alone, b) add NO2- alone, c) add N2O alone, d) add NO3 & NO2-, e) add NO3 & N2O, f) add NO2- & N2O, g) add NO3 , NO2- & N2O. The surface of the sediment was defined as depth 1 mm.

243x316mm (96 x 96 DPI)

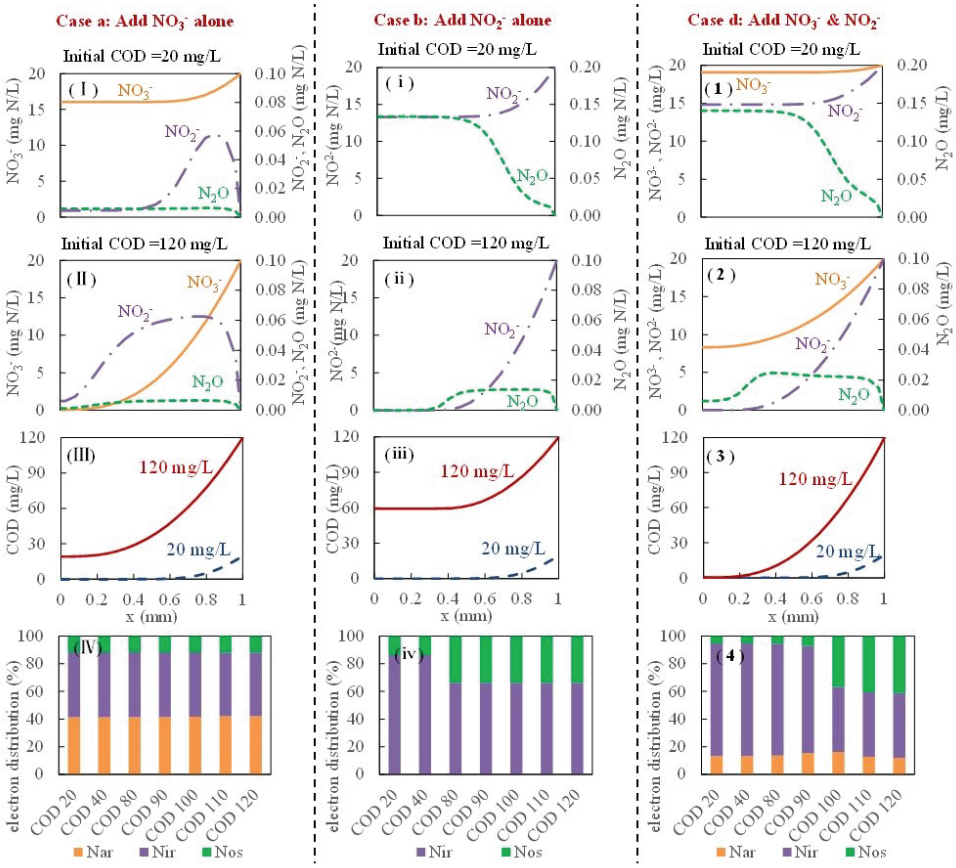

Figure 3. The effect of COD concentration on nitrogen oxides reduction (I~II, i~ii and 1~2), COD consumption (III, iii and 3), and electron distribution between Nar, Nir and Nos (IV, iv and 4). I~ IV show the simulation results of Case a, with only NO3 presenting in the influent. i~ iv show the simulation results of Case b, with only NO2− presenting in the influent. 1~4 show the simulation results of Case d, with both NO3 and NO2− in the influent. The surface of the sediment was defined as depth 1 mm.

263x237mm (96 x 96 DPI)

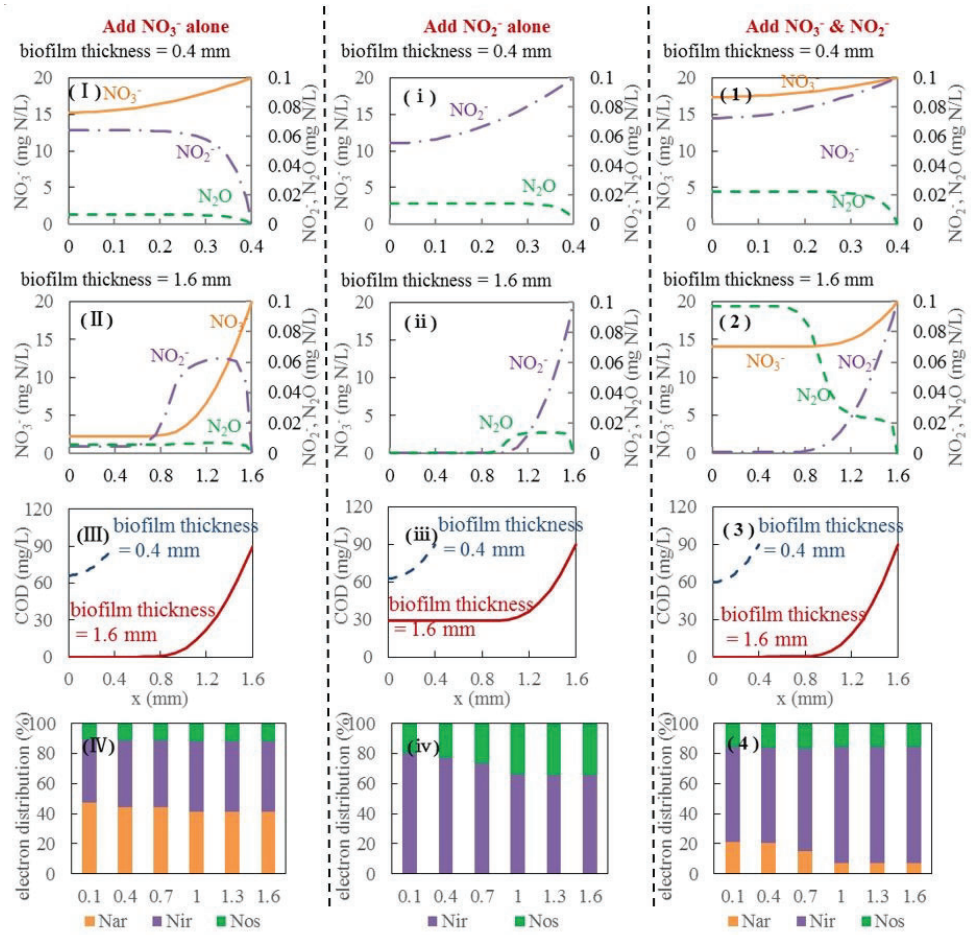

Figure 4. The effect of biofilm thickness on nitrogen oxides reduction (I~II, i~ii and 1~2), COD consumption (III, iii and 3), and electron distribution between Nar, Nir and Nos (IV, iv and 4). I~ IV show the simulation results of Case a, with only NO3 presenting in the influent. i~ iv show the simulation results of Case b, with only NO2− presenting in the influent. 1~4 show the simulation results of Case d, with both NO3 and NO2− in the influent. The bottom of the sediment was defined as depth 0 mm.

246x238mm (96 x 96 DPI)

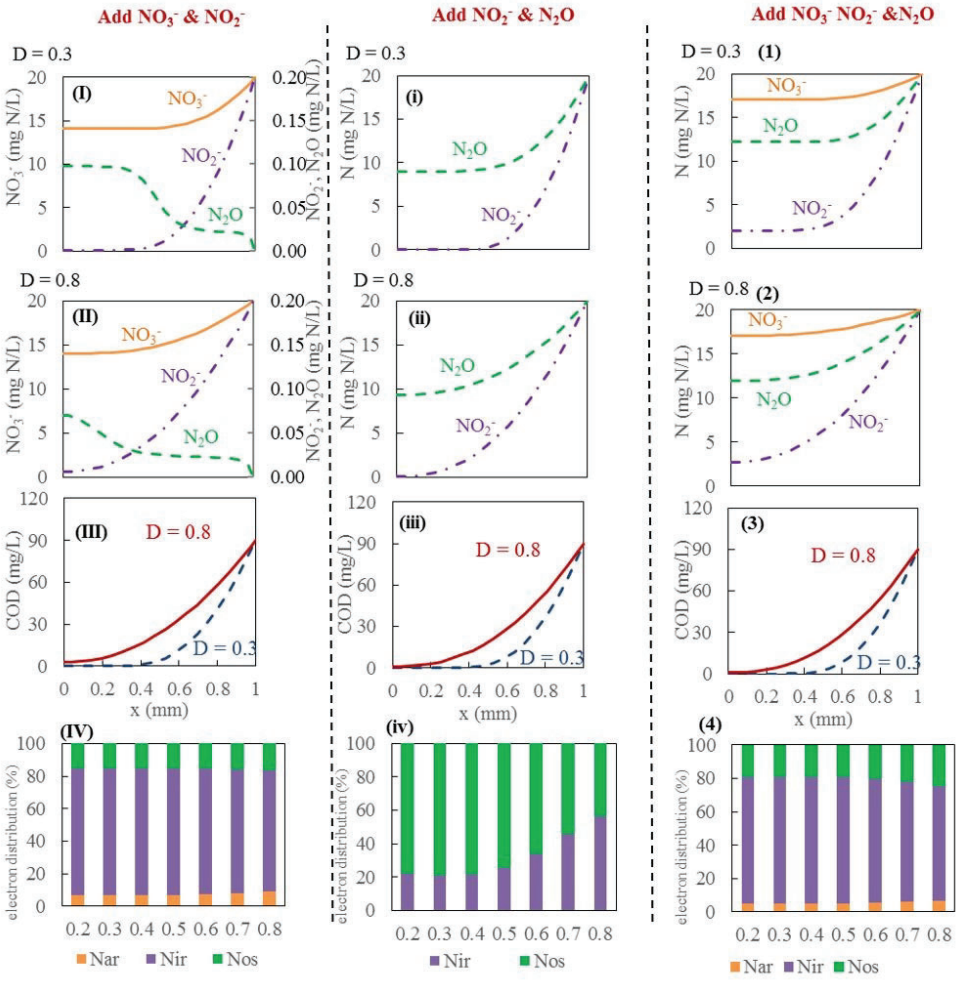

Figure 5. The effect of mass transfer on nitrogen oxides reduction (I~II, i~ii and 1~2), COD consumption (III, iii and 3), and electron distribution between Nar, Nir and Nos (IV, iv and 4). I~ IV show the simulation results of Case d, with NO3 and NO2 presenting in the influent. i~ iv show the simulation results of Case f, with NO2 and N2O presenting in the influent. 1~4 show the simulation results of Case g, with NO3 , NO2 and N2O present in the influent. The surface of the sediment was defined as depth 1 mm.

263x270mm (96 x 96 DPI)